

Mechanism of Sequence-Specific Fluorescent Detection of DNA by *N*-Methyl-imidazole, *N*-Methyl-pyrrole, and β -Alanine Linked Polyamides

Victor C. Rucker, Alexander R. Dunn, Shantanu Sharma, Peter B. Dervan, and Harry B. Gray*

Division of Chemistry and Chemical Engineering and the Beckman Institute, California Institute of Technology, Pasadena, California 91125

Received: November 10, 2003; In Final Form: March 8, 2004

The fluorescence from the tetramethylrhodamine (TMR) moiety in hairpin polyamide–TMR conjugates is quenched in solution, but restored upon sequence-specific binding to doubled-stranded DNA. This fluorescence amplification when bound to the target DNA sequence makes polyamide–TMR conjugates potentially useful for the detection of specific DNA sequences in homogeneous solution. Time-resolved and steady-state spectroscopic measurements indicate that a ground-state complex forms between the TMR and polyamide functionalities in the absence of DNA. This intramolecular complex likely facilitates electron transfer from the polyamide *N*-methyl-pyrrole moieties to the TMR excited state, quenching fluorescence. Binding of the polyamide–TMR probe to the target DNA sequence disrupts the TMR–polyamide interaction, resulting in the observed fluorescence increase.

Introduction

Hairpin polyamides are synthetic ligands that recognize the minor groove of double-stranded DNA with high affinity and sequence specificity.¹ As previously reported, the fluorescence of tetramethylrhodamine (TMR) is efficiently quenched when covalently attached to the ring nitrogen of a pyrrole residue within a polyamide.² Remarkably, the TMR fluorescence is restored when the polyamide–fluorophore conjugate binds to double-stranded DNA. The fluorophore remains quenched if the DNA does not contain the polyamide's match recognition site, indicating that the restoration of fluorescence results from sequence-specific binding in the minor groove.

We have made both steady-state and time-resolved luminescence measurements on the TMR–polyamide conjugates **1–4** in an attempt to understand this remarkable sequence-specific luminescence enhancement (Chart 1). In addition, the intermolecular interactions of the TMR fluorophore **10** with the polyamide fragments **6–9** (Chart 1) were examined using steady-state absorption and fluorescence spectroscopies. Our results indicate that TMR quenching in conjugates **1–4** is mediated by intramolecular hydrophobic interactions between the TMR and polyamide. We suggest electron transfer from the polyamide, most likely from a *N*-methyl-pyrrole moiety, to the singlet excited state of the fluorophore as a plausible quenching mechanism.

Experimental Procedures

All samples used in time-resolved studies were prepared in phosphate buffered Milli-Q water (10 mM Na₂HPO₄ pH 7.0, passed through a 0.2 μ m filter; ionic strength 19 mM). Samples used for measuring steady-state spectra were prepared in tris-EDTA buffered Milli-Q water: 10 mM Tris-HCl, 1 mM EDTA, adjusted to pH 7.4, and passed through a 0.2 μ m filter; calculated

ionic strength is 13 mM. The sequences of the TMR–conjugate recognition sites within the hairpin-forming DNA oligomers are **1**, 5'-taGTACtt-3'; **2**, 5'-taGTGTtt-3'; **3**, 5'-taGGTA-tt-3'; and **4**, 5'-taGCGCtt-3'. Each six-base recognition site is embedded in the stem of a 37-mer designed to form a DNA hairpin.²

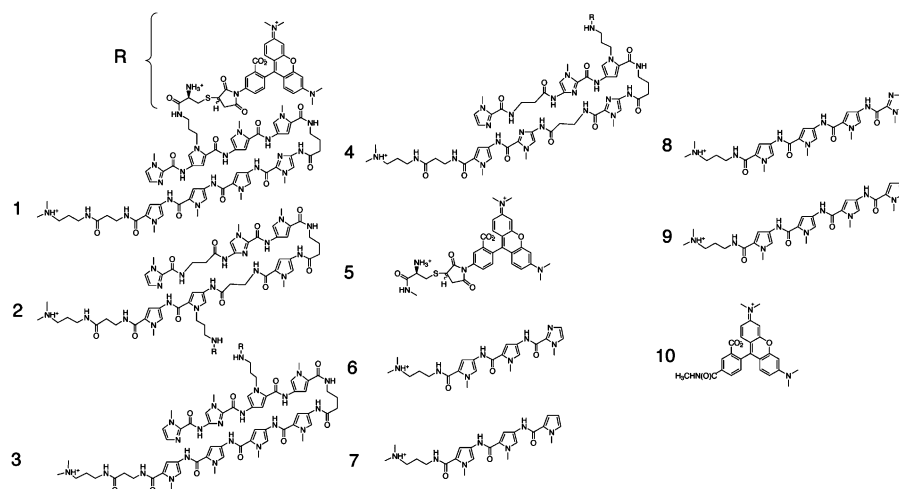
Time-resolved fluorescence kinetics were recorded with a Hamamatsu C5680 streak camera using the third harmonic (290 nm) of a regeneratively amplified femtosecond Ti:sapphire laser (Spectra-Physics) for the excitation pulse.³ Steady-state fluorescence spectra were collected on a Hitachi F-2500 fluorometer with samples excited at 545 nm. Absorption spectra were collected on a HP1045 absorption spectrometer. All samples were purged with argon for time-resolved spectroscopy. Quantum yield measurements were made relative to sulforhodamine 101.⁴ DNA was synthesized by Genbase, Inc. (San Diego, CA) and stored as previously described.² Cuvettes were from Starna.

Compounds **1–5** were synthesized as previously reported.^{2,5} 5-Carboxy-tetramethylrhodamine succinimidyl ester was reacted with methylamine to provide **10** after preparatory HPLC purification. Compounds **6–9** were prepared using oxime resin and also purified by preparatory HPLC. Compositions of all compounds were verified by MALDI/TOF mass spectrometry and analytical HPLC. For **6** (monoisotopic) [M + H] 456.67 (455.25 calcd for C₂₂H₃₁N₈O₃); **7** (monoisotopic) [M + H] 455.38 (454.26 calcd for C₂₃H₃₂N₇O₃); **8** (monoisotopic) [M + H] 578.85 (577.30 calcd for C₂₈H₃₇N₁₀O₄); **9** (monoisotopic) [M + H] 577.20 (576.30 calcd for C₂₉H₃₈N₉O₄); **10** (monoisotopic) [M + H] 444.54 (443.18 calcd for C₂₆H₂₅N₃O₄).

The streak camera response function was determined using scattered light from buffered water. Luminescence decay kinetics were determined for compounds **1–4** in the presence and absence of match DNA. Luminescence decay kinetics for **5** were collected in phosphate buffered Milli-Q water. The kinetics were analyzed by maximum entropy fitting (ME) as previously described.³ All data reported are the average of at least three determinations.

* Corresponding author. E-mail: hbgray@caltech.edu.

CHART 1: Structures of 1–10: R Indicates the TMR Moiety Abbreviated in 2–4



Results

Compounds 1–5. We observe monophasic luminescence decay for **5** with a lifetime of 4 ns (Figure 1). Conjugates **1–4** show biphasic luminescence decays in the absence of match DNA (Figure 1, –DNA), and ~90% monophasic decay with lifetimes identical to that of **5** upon binding match DNA (Figure 1, +DNA). In Figure 2, we show the rate constant (k) distribution for **1** in the presence and absence of match DNA. The rates cluster with mean lifetimes of 4 and 1.3 ns. Rate constant weightings [$P(k)$] for conjugates **1–4** in the presence and absence of DNA, and the monophasic decay from control **5**, are set out in Table 1. Binding of the fluorescent probe molecules to the target DNA sequences results in a modest decrease in the weighting of the fast phase of luminescence decay from ~30 to ~10%.

Quantum yields for the conjugates are **1**, 0.009; **2**, 0.04; **3**, 0.01; **4**, 0.03 in the absence of DNA. Upon binding match DNA, the quantum yields increase dramatically: **1**, 0.52; **2**, 0.50; **3**, 0.57; **4**, 0.38. The quantum yield for **5**, the TMR control compound, is 0.71. Importantly, the discrepancy between the modest changes in the lifetime distributions and the significant fluorescence increases upon polyamide binding in the minor groove of DNA suggests that a very rapid, unresolved decay pathway is responsible for the majority of TMR quenching in the absence of DNA.

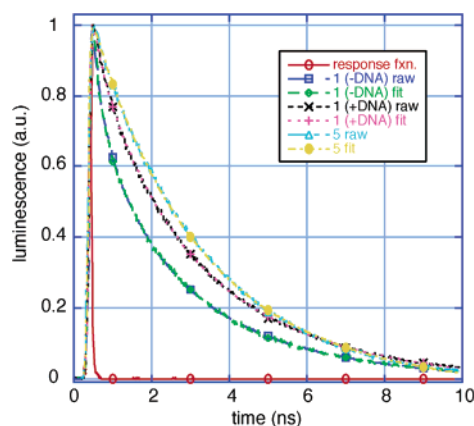


Figure 1. Observed and fitted luminescence decay kinetics for control **5**, and 3 μM **1** in the absence (–DNA) and presence (+DNA) of 6 μM match DNA. The decay of **1** in the presence and absence of DNA is representative of the general behavior of the other conjugates **2–4** under identical conditions.

TABLE 1: $P(k)$ Distribution for 1–5 in the Absence of DNA (A) and for 1–4 When Bound to Match DNA (B)^a

A	–DNA	$\Sigma P(k_{\text{fast}})^b$	$\Sigma P(k_{\text{slow}})^c$	$\frac{\Sigma P(k_{\text{fast}})}{\Sigma P(k_{\text{fast}}) + \Sigma P(k_{\text{slow}})}$	τ_{fast} (ns)	τ_{slow} (ns)
	1	0.38	0.85	0.31	1.3	4
	2	0.28	0.89	0.24	1.3	4
	3	0.42	0.76	0.34	1.3	4
	4	0.32	0.73	0.27	1.3	4
	5	n/a	1.13	n/a	n/a	4

B	+DNA	$\Sigma P(k_{\text{fast}})$	$\Sigma P(k_{\text{slow}})$	$\frac{\Sigma P(k_{\text{fast}})}{\Sigma P(k_{\text{fast}}) + \Sigma P(k_{\text{slow}})}$	τ_{fast} (ns)	τ_{slow} (ns)
	1	0.11	1.02	0.10	1.3	4
	2	0.11	1.05	0.09	1.3	4
	3	0.18	0.97	0.16	1.3	4
	4	0.10	1.08	0.09	1.3	4

^a All values are the average of three determinations. ^b Sum of the rate constant weightings $P(k)$ clustering around $\tau = 1.3$ ns. ^c Sum of the rate constant weightings $P(k)$ clustering around $\tau = 4.0$ ns.

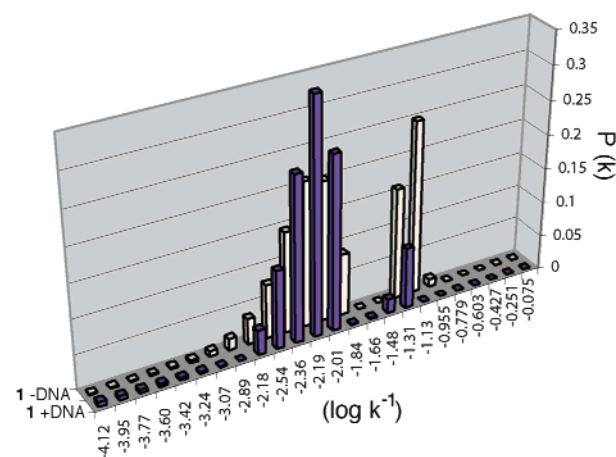


Figure 2. ME rate constant distribution for **1** in the absence (–DNA) and presence (+DNA) of match DNA. The time constants (k^{-1}) are given with units of 10 ns.

Dilution of solutions of **1–4** (~3 μM to ~40 nM) in the absence of DNA resulted in a decrease in the fluorescence intensity at 578 nm that was linearly dependent on the concentration of conjugate (Figure 3). These data indicate that the observed quenching is unlikely to result from fluorophore aggregation. Indeed, the linear decrease in fluorescence points to an intramolecular quenching mechanism.

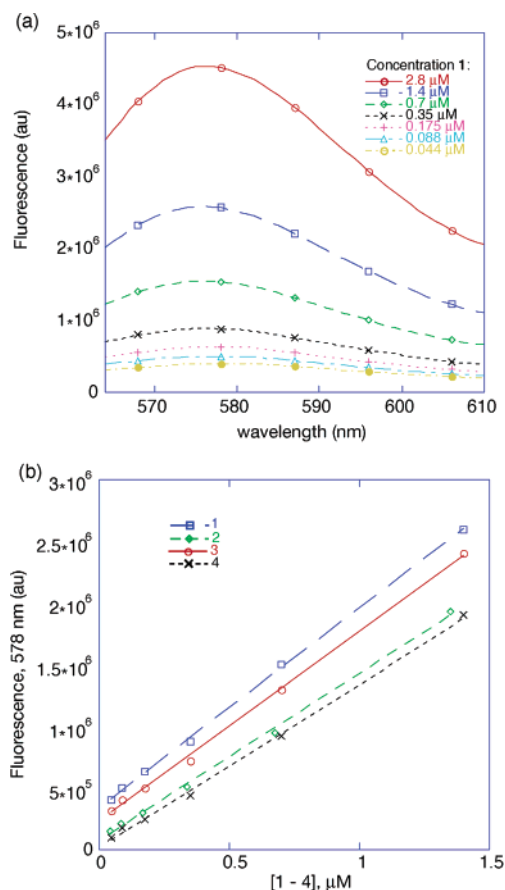


Figure 3. (a) Dilution of **1** from 1.4 μM to 44 nM. (b) Fit of linear decrease in fluorescence for **1–4**.

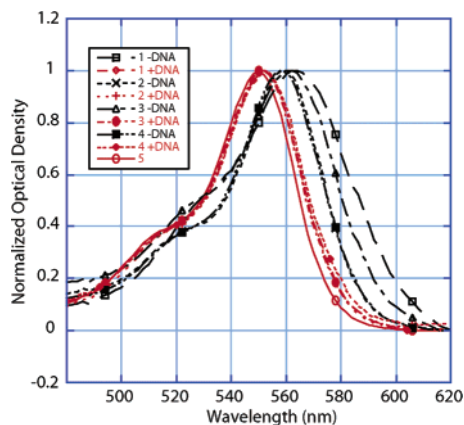


Figure 4. Steady-state absorption spectra of **1–4** in the absence (black lines) and presence (red lines) of match DNA. Control **5** also is shown.

The steady-state absorption spectrum of a chromophore may be perturbed in the presence of molecules that interact with it in the ground state.^{6–11} We observe pronounced bathochromic shifts in the absorption spectra of **1–4** as compared to **5**, a phenomenon noted for ground-state interactions involving the related xanthene fluorophore fluorescein.¹² There is a marked blue-shift upon binding of the polyamide to match DNA (Figure 4). Note that this hypsochromic shift almost exactly overlaps the TMR absorption of **1–4** with the absorption spectrum of control **5**. This behavior suggests that the ground-state interaction between the TMR and the polyamide is disrupted upon DNA binding, presumably by sequestration of the polyamide in the minor groove. The ground state TMR–polyamide interaction, together with the inference of an extremely rapid

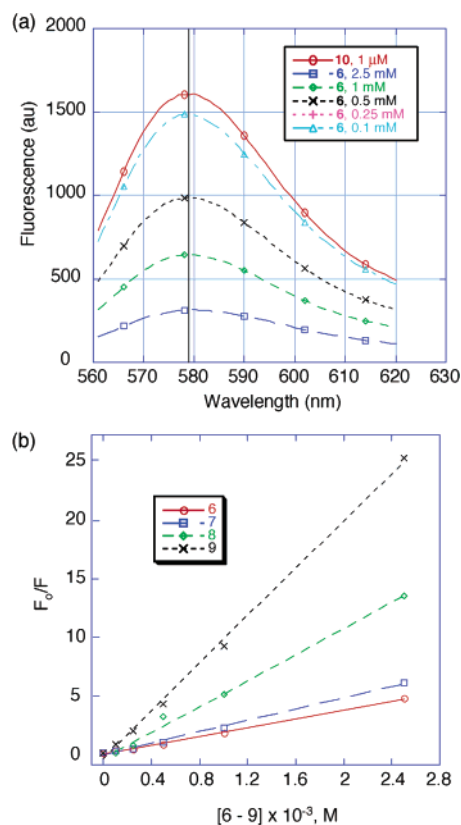


Figure 5. (a) Emission spectrum of 1 μM **10** in the presence of increasing concentration of quencher **6**. Note the invariance in emission maximum as shown by black line. (b) Fit of ratio of fluorescence from **10** in absence (F_0) and presence (F) of increasing concentration of polyamide quenchers **6–9**.

TABLE 2: Values of Quenching Association Constant, Emission Maximum, and Absorption Values for the Association of 6–9 with a 1 μM Concentration of 10^a

	$K_q \times 10^{-3} (\text{M}^{-1})$	$\text{Em}_{\text{max}}^b (\text{nm})$	$\text{Abs}_{\text{max}}^c (\text{nm})$	ΔAbs^d
6	1.88	578–580	562 , 554, 552	10
7	2.41	578–580	562 , 554, 552	10
8	6.48	578–580	566 , 556, 554	12
9	10.11	578–580	568 , 556, 556	14
10	n/a	578–580	552 , 554, 552	n/a

^a All values are the average of three determinations. ^b Note invariance in emission maximum. ^c First column indicates maximum bathochromic shift observed in aqueous solution for concentrations shown in Figure 6, second column represents absorption values in 50% (v/v) DMSO/water, and third column represents absorption values in 50% (v/v) methanol/water. ^d These are the maximum observed shifts in absorption observed under these experimental conditions. “n/a” indicates a nonapplicable column heading for **10**.

TMR quenching pathway, suggest that a static quenching mechanism likely accounts for the observed fluorescence quenching in the absence of DNA.

Compounds 6–10. A 1 μM solution of **10** was excited at 545 nm in the presence of 0.1, 0.25, 0.5, 1, and 2.5 mM **6–9**. We observe a linear decrease in fluorescence as the concentration of any given polyamide fragment **6–9** is increased (Figure 5a,b). Fitting the ratio of fluorescence from **10** in the absence of polyamide (F_0) and presence of polyamide (F) to the Stern–Volmer equation for static quenching ($F_0/F = 1 + K_q[Q]$) gives reasonable quenching association constants K_q for the interactions of **6–9** with **10** (Table 2). In contrast, fitting the data to a dynamic quenching model ($F_0/F = 1 + k_q\tau_0[Q]$), where τ_0 is the luminescence lifetime of **10** and k_q is the bimolecular quenching rate constant, results in calculated values of k_q that

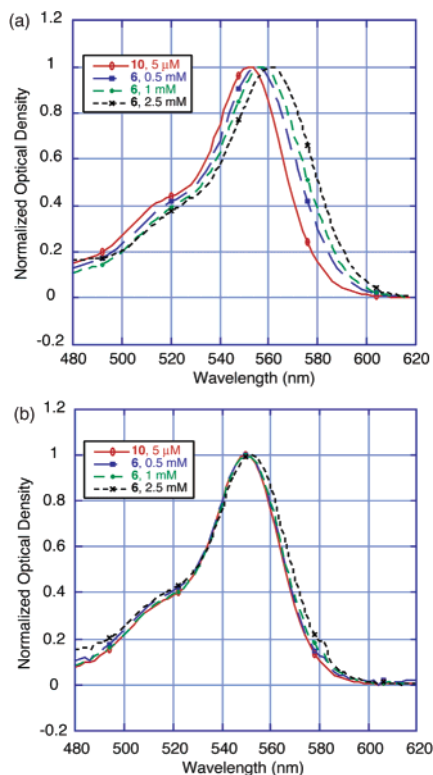


Figure 6. (a) Steady-state absorption spectra of $5 \mu\text{M}$ **10** with increasing concentrations of **6**. (b) Steady-state absorption spectra of **10** in 50% (v/v) methanol/ H_2O in the presence of identical concentration gradient used in panel a. Note that organic solvent abrogates the red shift observed in aqueous solution.

are larger than the maximum rates allowed by diffusion ($k_q > 10^{10} \text{ M}^{-1} \text{ s}^{-1}$).¹³ We also note invariance in the fluorescence maximum of **10** with increasing concentrations of **6–9**, a result consistent with a nonemissive TMR–polyamide complex.^{8,14–17}

The steady-state absorption spectra of $5 \mu\text{M}$ **10** with increasing concentrations of **6–9** exhibit a large concentration-dependent bathochromic shift (Figure 6a, Table 2). We suggest once again that this spectral shift is the product of a ground-state interaction between **10** and the polyamide. In contrast, no change in the absorption spectrum of **10** is observed when solutions are made using 50% (v/v) methanol (Figure 6b) or dimethyl sulfoxide as added organic cosolvent. Presumably, the organic cosolvents disfavor hydrophobic interactions between **10** and the polyamides, thus preventing association.

Conclusions

Interest in nondenaturing means for the sequence specific fluorescence detection of DNA has prompted us to undertake photophysical studies to further our understanding of how the fluorophore TMR is quenched when covalently attached to a DNA binding hairpin polyamide. We hypothesize that an intramolecular complex forms in the ground state between the fluorophore and the hairpin polyamide to which it is attached. Upon excitation, $>90\%$ of the molecules are rapidly quenched (<200 ps). Much smaller populations undergo luminescence decays with lifetimes of 4 and 1.3 ns, possibly indicating conformational or protonation heterogeneity within the conjugate sample.^{18,21} Sequestration of the polyamide in the minor groove physically prevents the intramolecular polyamide–fluorophore association essential for quenching (Figure 7).

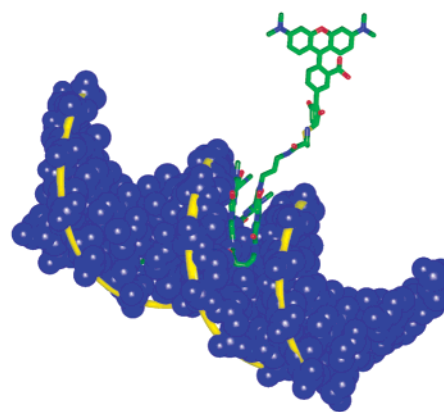


Figure 7. Model of the polyamide:TMR conjugate **1** (green, carbon; blue, nitrogen; yellow, sulfur; red, oxygen) docked into the minor groove of DNA (blue, space filling). Sequestration of the polyamide within the minor groove prevents intramolecular quenching of the TMR excited state.

The lack of spectral overlap between the TMR emission and polyamide absorption spectra precludes a Förster energy transfer quenching mechanism. In contrast, the oxidizing power of the excited TMR fluorophore ($E_{\text{red}}^{\text{ox}(\ast)} = 1.4 \text{ V vs NHE}$)^{10,19,22} could allow a proximate reductant to quench TMR fluorescence. We suggest that *N*-methyl pyrrole groups (E_{ox} measured $\sim 1 \text{ V vs AgCl/Ag}$; $\sim 1.2 \text{ V vs NHE}$)²⁰ in the polyamide reduce the TMR excited state through photoinduced electron transfer. Reductive quenching of xanthene fluorophores similar to TMR by nucleobases has been previously observed,^{10,19} and extremely short lifetimes, as proposed here, have been observed for electron-transfer quenching of fluorescein complexed with anticalin.¹¹

Acknowledgment. We wish to thank Dr. J. R. Winkler for assistance with data fitting and helpful discussions. This work was supported by the NSF (H.B.G.), National Institutes of Health (V.R.; training grant GM19789-02) and by the Fannie and John Hertz Foundation (A.R.D.).

References and Notes

- (1) Dervan, P. B. *Bioorg., Med. Chem.* **2001**, *9*, 2215.
- (2) Rucker, V. C.; Foister, S.; Melander, C.; Dervan, P. B. *J. Am. Chem. Soc.* **2003**, *125*, 1195.
- (3) Lyubovitsky, J. G.; Gray, H. B.; Winkler, J. R. *J. Am. Chem. Soc.* **2002**, *124*, 5481.
- (4) Karstens, T.; Kobs, K. *J. Phys. Chem.* **1980**, *84*, 1871.
- (5) Belitsky, J. M.; Nguyen, D. H.; Wurtz, N. R.; Dervan, P. B. *Bioorg., Med. Chem.* **2002**, *10*, 2767.
- (6) Johansson, M. K.; Fidler, H.; Dick, D.; Cook, R. M. *J. Am. Chem. Soc.* **2002**, *124*, 6950.
- (7) Armitage, B.; Retterer, J.; O'Brien, D. F. *J. Am. Chem. Soc.* **1993**, *115*, 10786.
- (8) Lakowicz, J. R. *Principles of Fluorescence Spectroscopy*, 2nd ed.; Kluwer Academic/Plenum Publishers: New York, 1999.
- (9) Schenk, G. H. *Absorption of Light and Ultraviolet Radiation: Fluorescence and Phosphorescence Emission*; Allyn and Bacon, Inc.: Boston, 1973.
- (10) Seidel, C. A. M.; Schulz, A.; Sauer, M. H. M. *J. Phys. Chem.* **1996**, *100*, 5541.
- (11) Götz, M.; Hess, S.; Beste, G.; Skerra, A.; Michel-Beyerle, M. E. *Biochemistry* **2002**, *41*, 4156.
- (12) Voss, E. W., Jr.; Croney, J. C.; Jameson, D. M. *J. Protein Chem.* **2002**, *21*, 231.
- (13) Tinoco, I., Jr.; Sauer, K.; Wang, J. C.; Puglisi, J. D. *Physical Chemistry: Principles and Applications in Biological Sciences*; Prentice Hall: New Jersey, 2002.
- (14) Nemzek, T. L.; Ware, W. R. *J. Chem. Phys.* **1975**, *62*, 477.
- (15) Eftink, M. R.; Ghiron, C. A. *J. Phys. Chem.* **1976**, *80*, 486.
- (16) Rabinowitch, E.; Epstein, L. F. *J. Am. Chem. Soc.* **1941**, *63*, 69.

- (17) Kubota, Y.; Motoda, Y.; Shigemune, Y.; Fujisaki, Y. *Photochem. Photobiol.* **1979**, 29, 1099.
- (18) Edman, L.; Mets, Ü; Rigler, R. *Proc. Natl. Acad. Sci. U.S.A.* **1996**, 93, 6710.
- (19) Torimura, M.; Kurata, S.; Yamada, K.; Yokomaku, T.; Kamagata, Y.; Kanagawa, T.; Kurane, R. *Anal. Sci.* **2001**, 17, 155.
- (20) Kim, O.-K.; Hu, H. S. W.; Lee, Y. S. *Mol. Cryst. Liq. Cryst.* **1990**, 190, 9. The reported N-methyl pyrrole potential is irreversible, and therefore has a large uncertainty.
- (21) Wennmalm, S.; Edman, L.; Rigler, R. *Proc. Natl. Acad. Sci. U.S.A.* **1997**, 94, 10641.
- (22) Yasui, S.; Tsujimoto, M.; Itoh, K.; Ohno, A. *J. Org. Chem.* **2000**, 65, 4715.